Food Chemistry: X 24 (2024) 101901

Contents lists available at ScienceDirect

Food Chemistry: X

journal homepage: www.sciencedirect.com/journal/food-chemistry-x

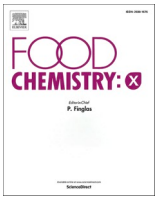

Ultrasonic depolymerization of pomegranate peel pectin: Effect of sonication time on antioxidant, α-amylase inhibitory, and prebiotic properties

Sahar Bachari [a], Maryam Ghaderi-Ghahfarokhi [a,*], Hassan Ahmadi Gavlighi [b,c], Mehdi Zarei [a]

[a] Department of Food Hygiene, Faculty of Veterinary Medicine, Shahid Chamran University of Ahvaz, Ahvaz, Iran
[b] Department of Food Science and Technology, Faculty of Agriculture, Tarbiat Modares University, Tehran, Iran
[c] Halal Research Center of IRI, Iran Food and Drug Administration, Ministry of Health and Medical Education, Tehran, Iran

ARTICLE INFO

Keywords:
α-Amylase inhibition
Antioxidant activity
Prebiotic activity
Pectin
Pomegranate peel
Ultrasonic treatment

ABSTRACT

This study aimed to investigate the effects of ultrasonic treatment time (5–30 min) on the structural characteristics, antioxidant, α-amylase inhibitory, and prebiotic properties of pomegranate peel pectin (PPP). The extracted PPP was rich in galacturonic acid (64.27 %) and exhibited a high degree of esterification (DE, 61.7 %), with an average molecular weight (*Mw*) of 135.6 kDa. The *Mw*, particle size, and DE of ultrasonic-treated PPPs (U-PPPs) significantly decreased compared to the PPP. FTIR analysis revealed that the intensity of the peak at ~1730–1720 cm^{-1} weakened with prolonged treatment time. The total phenol content, antioxidant activity, and α-amylase inhibition of U-PPPs were enhanced compared to PPP. Both PPP and U-PPP treated for 30 min promoted the growth of *Bifidobacterium longum* and *Lactobacillus casei*, with U-PPP-30 showing a greater preference over PPP and inulin. In conclusion, ultrasonic treatment represents a promising approach to depolymerization aimed at enhancing the biological activities of pectin.

1. Introduction

Pomegranate (*Punica granatum*) peel (PP), a by-product of the juice processing industry, accounts for 50–55 % of the fruit's weight. It contains a range of valuable substances, including pectin, phenolic compounds (10–20 %), and lignocellulosic matter (40–50 %) (Abid et al., 2017; Sharifi et al., 2022). Due to the increased production and processing of pomegranates, large quantities of PP are discarded annually. Consequently, it holds significant potential for valorization into various commercial products through integrated processes.

Pectin, a heteropolysaccharide found in plant cell walls, is primarily composed of three major blocks: homogalacturonan (HG, 65 %), rhamnogalacturonan-I (RG-I, 20–30 %), and rhamnogalacturonan-II (RG-II, 1–8 %) (Ogutu & Mu, 2017). Due to its unique structure, pectin exhibits numerous technological properties and is utilized in diverse food products as a gelling agent, emulsifier, thickener, texturizing agent, fat replacer, and stabilizer (Muñoz-Almagro et al., 2017; Qiu, Cai, et al., 2019). Additionally, an increasing number of studies have reported the health-promoting properties and bioactivities of pectin, including anti-tumor, anti-inflammatory, immunoregulatory, antibacterial, prebiotic, hypoglycemic, and antioxidant effects, thereby opening new application opportunities in the pharmaceutical field (Minzanova et al., 2018).

Despite pectin's promising technological and biomedical potential, its complex structure, high viscosity, poor solubility, and high molecular weight hinder its effectiveness. To address these inherent drawbacks, various methods for modifying pectin have been developed (Chen et al., 2019; Qiu, Cai, et al., 2019; Yan et al., 2021). Among the different modification methods, pectin depolymerization is the most popular, typically achieved through enzymatic or chemical (e.g., hydrogen peroxide, acid, and alkali) hydrolysis. However, these methods have encountered several limitations, such as high costs, time-consuming procedures, uncontrollable changes in molecular weight, environmental concerns, and complex processing requirements (Yan et al., 2021). Therefore, exploring a cost-effective, environmentally friendly, and efficient method is crucial for improving its functionality while broadening its biological and technological applications.

Ultrasonic power (20-100 kHz) has been adopted as a sustainable, innovative, and green technique for manipulating the molecular weight of polysaccharides (Qiu, Zhang, & Wang, 2019; Zhang, Ye, Ding, et al.,

* Corresponding author at: Department of Food Hygiene, Faculty of Veterinary Medicine, Shahid Chamran University of Ahvaz, PO Box 6135783151, Ahvaz, Iran.
E-mail address: m.ghaderi@scu.ac.ir (M. Ghaderi-Ghahfarokhi).

https://doi.org/10.1016/j.fochx.2024.101901
Received 31 August 2024; Received in revised form 2 October 2024; Accepted 11 October 2024
Available online 14 October 2024

2013). It is regarded as an alternative or complement to conventional chemical and enzymatic methods for reducing molecular weight. This approach offers a robust and promising means to regulate the degree of depolymerization, enhance yield, shorten processing time, and prevent unwanted reactions (Muñoz-Almagro et al., 2017). Recent studies have explored the use of ultrasound irradiation for modifying pectin extracted from various sources, such as hawthorn wine pomace (Chen et al., 2019), citrus (Yan et al., 2021), citrus and apple (Muñoz-Almagro et al., 2017), sweet potato (Ogutu & Mu, 2017), and mushroom (*Auricularia auricula*) (Qiu, Zhang, & Wang, 2019).

It is well-established that pectic-oligosaccharides (POSs) obtained from depolymerized pectin possess superior bioactivities compared to intact pectin. POSs are recognized as prebiotics that may improve human health by selectively fermenting and supporting beneficial gut bacteria, facilitating changes in bacterial populations that are either comparable to or superior to those achieved with commercial prebiotics like galacto- and fructooligosaccharides (Zhang et al., 2018; Zhu et al., 2019). Moreover, ultrasonic-modified polysaccharides can serve as a new source of antioxidants (Chen et al., 2019; Ogutu & Mu, 2017), hypoglycemics agents (Xu et al., 2018), and other promising therapeutic benefits.

Research on pomegranate peel pectin (PPP) has primarily focused on its extraction, composition, structure, and functional properties (e.g., emulsifying, viscosity, and gel formation) (Abid et al., 2016; Abid et al., 2017; Yang et al., 2018). Iran stands as one of the largest producers of pomegranates, resulting in a substantial amount of peel waste generated annually by processing industries. This presents a significant opportunity to explore the extraction of pectin from these peels and further process it into POSs with various biological activities. Previous studies have highlighted that pectin derived from pomegranate peels exhibits immunomodulatory activity (Gavlighi et al., 2018). However, there has been a lack of research specifically investigating the antioxidant, α-amylase inhibitory, and prebiotic activities of PPP and its derived POSs. This study addresses this gap by representing the first attempt to depolymerize PPP using ultrasonic radiation. The physicochemical characteristics and bioactivities of the resulting ultrasonic-degraded PPPs (U-PPPs) were investigated in comparison to native PPP, with a specific focus on their antioxidant effects, α-amylase inhibitory activity, and prebiotic potential.

2. Material and methods

2.1. Plant material and reagents

Mature pomegranate fruits were sourced from a local store. After being washed, the peels were manually removed and then sliced into small fragments. The peels were then oven-dried (Model E240, Binder GmbH, Germany) at 45 ± 1 °C for 36 h. The dried PP was crushed using an Artisan grinder (model 5000, Sina Tajhiz Co. Iran) and sieved through a 40-mesh filter. The resulting powder was then sealed in polyethylene bags and stored at −18 °C. The proximate composition of pomegranate peel powder (crude protein, crude fiber, ash, total carbohydrate, moisture, and fat contents) was measured according to the standard methods of AOAC (2019).

All culture media for microbiological analysis, including de Man Rogosa Sharpe (MRS) broth, MRS agar, trypticase soy agar (TSA), and trypticase soy broth (TSB), were supplied by Ibresco (Zist Kavosh Iranian Company, Karaj, Iran). Monosaccharide standards (*D*-arabinose, *L*-fucose, *D*-glucose, *L*-rhamnose, *D*-galactose, *D*-xylose, *D*-mannose, and *D*-galacturonic acid), Folin-Ciocalteu reagent, gallic acid, 1,1-diphenyl-2-picrylhydrazyl (DPPH) radicals, 2,4,6-Tris(2-pyridyl)-*s*-triazine (TPTZ), *L*-cysteine, porcine pancreatic α-amylase (Cat no. A3176) were purchased from Sigma–Aldrich Chemical Co. (St. Louis, USA). Also, $FeCl_3$, $FeSO_4.7H_2O$, PAHBAH (4-hydroxybenzohydrazide) and soluble starch ACS reagents were supplied by Merck (Darmstadt, Germany). All solvents and chemicals were of analytical grade.

2.2. Extraction of pectin from pomegranate peel

Pectin extraction was carried out based on the method of Gavlighi et al. (2018) with some modifications. PP powder was mixed thoroughly with distilled water (1 : 50 by wt.) until a complete suspension was achieved. The pH of the suspension was adjusted to 1.5 ± 0.5 with HCl (1 N), and the mixture was heated at 90 °C for 90 min in a water bath (Fan Azma Gostar, Karaj, Iran). After cooling, the suspension was centrifuged (Model TL 320, Selecta lab, Spain) at 2147*g* for 15 min. The supernatant was mixed with two volumes of cold ethanol (96 %) and kept at 4 °C overnight to allow the participation of pectin. The floating pectin gel was then drained by centrifugation at 2810*g* for 10 min at 4 °C. The extracted PPP was washed with ethanol and centrifuged repeatedly to aid dehydration. Finally, pectin was dried at 45 ± 1 °C, milled, and stored at −18 °C until use. The yield of pectin extraction from pomegranate peel was calculated as follows:

$$Y = M_{pectin} \times 100 / M_{peel} \quad (1)$$

where Y is the yield of pectin extraction from PP, M_{pectin} is the weight of extracted pectin (gr), and M_{peel} is the weight of the initial dried peel (gr) used for extraction. Also, the crude protein, moisture, and fat content of PPP were measured using the standard methods of AOAC (2019).

2.3. Ultrasonic degradation

PPP was degraded using an ultrasonic probe instrument (Model UP-100, ChromTech, Taiwan) operating at 20 kHz and with 100 W maximum output power. It was equipped with a horn probe with a 13 mm tip diameter. A stock solution of PPP was prepared (5 mg/ml) under constant stirring at 25 °C for 2 h. The dispersion was stored at 4 °C overnight to reach complete dissolution and hydration. The PPP solution (20 ml) was placed in conical flasks and subjected to pulsed ultrasound (5 s on and 5 s off period) at 80 W for 5, 10, 15, and 30 min in an ice bath. The probe was consistently adjusted to a fixed depth of 2 cm in the PPP solution. The resultant solutions were centrifuged for 30 min at 2147 *g* (Qiu, Cai, et al., 2019), and the supernatant was dried at 45 °C and kept at −18 °C for further experiments. The original PPP without ultrasonic modification was considered as control, and U-PPP-5, U-PPP-10, U-PPP-15, and U-PPP-30 were sonolyzed for 5, 10, 15, and 30 min, respectively.

2.4. Characterization of PPP and U-PPPs

2.4.1. Sugar composition

The sugar composition was analyzed by hydrolyzing samples with 2 M TFA at 120 °C for 2 h. The resulting hydrolysates were reduced by $NaBD_4$ and acetylated using acetic anhydride (Ac_2O). An ICS3000 ion chromatography system equipped with a GS50 gradient pump, CarboPacTM PA20 (3 mm × 150 mm) analytical column (Dionex Corp., Sunnyvale, CA), an ED50 electrochemical detector, and AS50 autosampler (Dionex Corp., Sunnyvale, CA) was employed for sample analysis (Gavlighi et al., 2013). The column re-equilibration was performed with 100 mM NaOH, followed by 2.5 mM NaOH, each for 5 min. The monosaccharides were effectively separated using a two-eluent system composed of aqueous NaOH (500 mM) and deionized water (18.2 mU at 25 °C), with adequate resolution. The eluent flow rate was set to 0.5 ml/min, with an injection volume of 10 μl. Neutral monosaccharides were eluted isocratically with NaOH (2.5 mM) for 20 min, followed by a second isocratic elution using NaOH (500 mM) for 10 min to elute acidic monosaccharides (Balaghi et al., 2011).

2.4.2. Determination of molecular weight

Freeze-dried samples (4 mg) were dissolved in distilled water (2 ml) and microwaved for 30 s using a microwave bomb model #4782 (Parr Instrument Co., Moline, IL, USA). Before injection, the samples were passed through a 3.0 μm cellulose acetate filter to eliminate large

contaminants and particles. The injection volume was 20 µl, and the mobile phase consisted of $NaNO_3$ (0.15 M) and NaN_3 (0.02 %), with a flow rate of 0.4 ml/min. The molecular weight of samples was analyzed by high-performance size-exclusion chromatography (HPSEC), composed of a TSK G5000 PW column (7.5 mm × 600 mm; TosoBiosep, Montgomeryville, PA, USA) coupled with UV detector (Waters, 2487), Multi-Angle Laser Light Scattering (HELEOS; Wyatt Technology Corp, Santa Barbara, CA, USA), and a refractive index detector (Waters, 2414) (HPSEC-UV-MALLS-RI). Bovine serum albumin (BSA) was used to determine the volume delays between the UV, MALLS, and RI detectors. The average molecular weight (*Mw*) was determined using ASTRA 5.3 software (Wyatt Technology Corp.) (Gavlighi et al., 2018).

2.4.3. Particle size and ζ-potential

The particle size and ζ-potential of samples were determined by dynamic light scattering (DLS) using a Zetasizer (Nano-S90, Malvern Instruments Ltd., Malvern, UK) at 632.80 nm and a 90° scattering angle. Three runs were conducted for each sample.

2.4.4. Degree of esterification (DE)

Pre-weighted PPP and U-PPPs (50 mg) were placed in an Erlenmeyer flask made wet with ethanol (1 ml), dissolved in deionized water (20 ml), and stirred at 40 °C for 30 min. After complete dissolution, the phenolphthalein indicator was added to the solution and titrated with NaOH (0.1 M) until the color turned pink (V1). Subsequently, 5 ml of NaOH solution (0.1 M) was added, and the solutions were stirred at room temperature. After 30 min, 5 ml of HCl (0.1 M) was added while stirring until the pink color faded. Lastly, the mixture was treated with a phenolphthalein indicator, and the solution was again titrated with NaOH (0.1 M) (V2) until the pink color reappeared (Chen et al., 2019). The DE was calculated using the following formula:

$$\mathrm{DE}\ (\%) = V_2 \times 100 / V_1 + V_2 \tag{2}$$

2.4.5. FTIR spectroscopy

PPP/U-PPP samples were mixed uniformly with KBr and pressed into transparent pellets before analysis. The FTIR spectra of samples were recorded using a Tensor II spectrometer (Bruker, Germany) in the wavenumber range of 400–4000 cm^{-1} with 16 scans at a resolution of 4 cm-1.

2.5. Color and turbidity

The absorbance of the PPP/U-PPPs solutions (0.5 % *w/v*) was measured at 480 nm using a UV–visible spectrophotometer (Cecil Instruments Ltd., Cambridge, UK). The color parameters of the PPP/U-PPPs solution (0.5 % w/v) were determined using the Colorflex EZ with the CIE LAB color system (Hunter Associates Laboratory, Virginia, United States). After calibration with a standard white plate ($L^* = 91.06$, $a^* = -0.96$, and $b^* = 1.43$), lightness (L^*), redness (a^*), and yellowness (b^*) values were measured in the CIE system, with three replications at ambient temperature. The total color difference (ΔE) was calculated for each sonication time relative to the control sample (PPP) using following equation:

$$\Delta E = \sqrt{[(\Delta L^*) + (\Delta b^*) + (\Delta a^*)]} \tag{3}$$

Where ΔL^*, Δb^*, and Δa^* are differences between the Hunter parameters of the PPP and each U-PPP sample (Bodart et al., 2008).

2.6. Antioxidant activity

2.6.1. Total phenolic content

The total phenolic content (TPC) of the samples was measured using the Folin-Ciocalteu assay, following the method of Zhang et al. (2016). Briefly, 125 µL of Folin-Ciocalteu reagent was added to 25 µL of pectin solution (5 mg/ml) in a 96-well microplate. After a 10-min incubation at room temperature, the samples were mixed with 125 µL of a 7.5 % (*w/v*) sodium carbonate solution. The absorbance of the test solution was recorded at 765 nm after incubation for 30 min at room temperature using a Synergy HT microplate reader (BioTek Instruments Inc., Winooski, VT, USA). Gallic acid served as the reference standard, and the results were reported as mg of GA equivalents per gram of sample. A gallic acid standard curve at a concentration of 25–800 µg/ml ($y = 0.0015\times + 0.0156$, $R^2 = 0.0999$) was used to calculate the TPC. The results were expressed as milligram gallic acid equivalents (mg GAE) per gram of dried PPP/U-PPPs.

2.6.2. Scavenging activity of DPPH radicals

The antioxidant activity of the samples was evaluated using a DPPH radical scavenging assay. Briefly, 100 µl of pectin solution (25–250 µg/ml) was added to the equal volume of DPPH methanolic solution (7.8 mg/100 ml) in a 96-well microplate. The prepared mixture was left in the dark for 30 min at 37 °C. The absorbance values were determined at 517 nm using a microplate reader after 30 min (Chen et al., 2019). DPPH solution without the tested PP/PPHs was considered as a control. The scavenging activity of the samples was calculated using the following formula:

$$\textit{Scavenging activity}\ (\%) = (A_c - A_s) \times 100 / A_c \tag{4}$$

where A_c is the absorbance of the control and A_s is the absorbance of the sample. Samples were analyzed in triplicate.

The FRAP assay was used to evaluate the ability of PPP/U-PPPs to reduce the ferric (Fe^{3+}:TPTZ complex) to its ferrous form (Fe^{2+}:TPTZ). To prepare the FRAP solution, acetate buffer solution (0.3 M, pH = 3.5), TPTZ (10 mM in 40 mM HCl), and $FeCl_3$ (20 mM) were mixed in a ratio of 25:5:5 (*v*/v). The prepared solution was kept at 37 °C for 30 min. Then, 2850 µl of FRAP solution was mixed with 150 µl of PPP/U-PPPs solutions at various concentrations (100–1000 µg/ml). The absorbance of the samples was recorded at 593 nm after 30 min incubation at 37 °C (Benzie & Strain, 1996). FRAP was determined using a standard curve of $FeSO_4.7H_2O$ (25–1000 mM) and expressed as µM of Fe^{2+} equivalents per mg of dried sample (µM Fe^{2+}/mg sample).

2.7. α-Amylase inhibitory activity

The inhibitory effect of PPP and U-PPPs against α-amylase activity was determined following the method of Mirab et al. (2020). The enzyme (2.5 U/ml) was dissolved in sodium phosphate buffer (0.02 mol/l, pH 6.9) containing 6.7 mmol/l NaCl. PPP and U-PPPs solutions were also prepared in sodium phosphate buffer at 10 mg/ml concentration. Then, PPP and U-PPPs (100 µl) and α-amylase solution (100 µl) were mixed thoroughly with α-amylase solution (100 µl), followed by incubation at 37 °C for 5 min. The starch solution (0.5 % *w/v*, 100 µL) was then added, and the resulting solution was incubated at 37 °C for 20 min. After enzyme deactivation (at 100 °C for 10 min), the solutions were centrifuged at 12282 *g* for 2 min to separate the undigested starch. PAHBAH reagent (1 ml) was added to the supernatant (20 µl) and incubated at 70 °C for 10 min. After cooling, absorbance was recorded at 410 nm using a UV–visible spectrophotometer (Carry 60, Agilent, US). The α-amylase inhibitory activity of the PPP and U-PPPs was calculated using the following formula:

$$\alpha - \textit{amylase inhibation}\ (\%) = A_c - (A_b - A_s) \times 100 / A_c \tag{5}$$

where A_s, A_b, and A_c are the absorbance of the sample, blank (phosphate buffer, α-amylase, and sample), and control (starch, phosphate buffer, and α-amylase), respectively. The IC_{50} value of acarbose was used as a control.

2.8. Evaluation of prebiotic activity

2.8.1. Bacterial strains

Two bacterial strains, *Bifidobacterium longum* (ATCC 55813) and *Lactobacillus casei* (ATCC 393) were employed to evaluate the in vitro prebiotic activity of PPP and U-PPP-30 samples. These strains were kindly provided by Pardis Roshd Mehregan (Shiraz, Iran). The stock cultures were stored in MRS broth containing 20 % (*v*/v) glycerol at −80 °C. The L. *casei* strain was cultured twice in MRS broth medium, while the *B. longum* strain was incubated anaerobically in MRS medium supplemented with *L*-cysteine (0.05 % *w/v*). Both strains were incubated at 37 °C for a duration of 24 h. The cells were collected using a centrifuge at 6000 ×*g* and 4 °C for 5 min, followed by washing twice with sterile normal saline solution and resuspending in an equal volume of normal sterile saline before inoculation (Zhou et al., 2018).

2.8.2. In vitro prebiotic test and acidifying activity of probiotics

Sugar-free Man-Rogosa-Sharp medium (SF-MRS) was prepared by mixing various ingredients in Milli-Q water, as reported by Moreno-Vilet et al. (2014). The pH of the medium was adjusted to 6.2 ± 0.2 and autoclaved at 121 °C for 15 min. After cooling, the SF-MRS broth medium was supplemented with 0.5 and 1 % w/v of inulin, PPP, and U-PPP-30 powder in individual bottles. SF-MRS was used as a negative control, while commercial MRS containing 2 % glucose and inulin served as the positive control and standard prebiotic, respectively. All prebiotic powders were sterilized using UV light (254 nm, 40 w) for 20 min, and sterility was verified using the total viable count on TSA before use. The SF-MRS bottles were inoculated individually with each probiotic strain at ~1×10^4 CFU/ml. The broth medium was then divided into test tubes and incubated at 37 °C for 48 h. Enumeration of probiotic strains was carried out on MRS agar medium at 24-h intervals, followed by incubation at 37 °C for 48 h. For *B. longum*, *L*-cysteine (0.05 %) was added to the medium. The population of probiotics was expressed as Log CFU/ml. Simultaneously, the utilization of different carbohydrate sources by the strains was assessed by determining the pH and titratable acidity (TA) of the media according to the standard method of AOAC (2019).

2.8.3. Prebiotic activity score (PAS)

Escherichia coli (ATCC 25922) was used as the representative enteric strain. Frozen stock culture (50 µl) of *E. coli* was inoculated onto sterilized TSA plates, which were then incubated at 37 °C for 48 h. Colonies were re-cultured in TSB, and an overnight culture of *E. coli* was used to determine the PAS. The M9 minimal broth medium was prepared according to Rubel et al. (2014) and supplemented individually with inulin, PPP, and U-PPP-30 at 1 % *w/v* in separate bottles. After inoculation with *E. coli* at 10^4 CFU/ml, cultures were incubated under the aerobic condition at 37 °C and plated on TSA after 24 h. The M9 medium without a carbohydrate source served as the negative control. Each assay was replicated three times. A PAS was calculated as follow:

$$PAS = \left(Log\, P_X^{24} - Log\, P_X^0 / Log P_G^{24} - Log\, P_G^0\right) - \left(Log\, E_X^{24} - Log\, E_X^0 / Log E_G^{24} - Log\, E_G^0\right) \quad (6)$$

where $P_G{}^0$, $P_X{}^0$, $P_G{}^{24}$, $P_X{}^{24}$ are the probiotic counts in the presence of glucose (G) and PPP-1 %/ U-PPP-30-1 %/inulin-1 % (X) at time 0 and 24 h. $E_G{}^0$, $E_X{}^0$, $E_G{}^{24}$, $E_X{}^{24}$ are the enteric counts in glucose (G) and PPP-1 %/U-PPP-30-1 %/inulin-1 % (X) at time 0 and 24 h.

2.9. Statistical analysis

Statistical analysis was performed using Minitab 16 software (Minitab Inc., State College, PA, USA). One-way analysis of variance (ANOVA) followed by Tukey's test was employed to compare the differences between samples and mean values, with a confidence level of $P < 0.05$. Results are reported as mean ± standard deviation (SD) from three independent replicates. For the prebiotic activity assay, the collected data were analyzed using the General Linear Model (GLM) procedure to examine the main effects of prebiotic type and fermentation time, as well as their interaction, on the probiotic population, pH, and TA values.

3. Results and discussion

3.1. Chemical composition of pomegranate peel and extracted pectin

The composition analysis revealed that the pomegranate peel contained 4.56 ± 0.17 % moisture, 3.36 ± 0.20 % total ash, 67.77 ± 0.89 % total carbohydrate, 3.27 ± 0.23 % crude protein, 19.62 ± 0.45 % crude fiber, and 1.49 ± 0.03 % of fat. Additionally, the extracted PPP was found to contain 1.87 ± 0.30 % protein and 3.45 ± 0.43 % moisture while being devoid of fat. These values differ from those observed in Tunisian pomegranate cultivars, where the ash, protein, and crude fiber contents of the peel ranged from 3.71 % to 4.97 %, 2.58 % to 7.13 %, and 27.11 % to 32.51 %, respectively (Abid et al., 2017). Furthermore, Gavlighi et al. (2018) reported a higher protein content compared to that of PPP in the present study, with values of 21.40 %, 39.58 %, and 15.05 % for pectin extracted using buffer, enzyme, and acid methods, respectively. The differences are likely due to the varied extraction methods and the distinct chemical characteristics of the initial material.

In this study, the extraction yield of pectin from PP was 9.42 ± 1.17 %. This value was higher than the yield of 8.93 ± 0.17 % reported by Sharifi et al. (2022) for pectin extracted from pomegranate peel using HCl as a solvent (pH = 1.5) at a solid-to-solvent ratio of 1:40 and a temperature of 86 °C. Our results align with those of Gavlighi et al. (2018), who reported a yield of 9.37 % for pomegranate pectin extracted under comparable conditions (pH ~ 1.5 at 90 °C for 90 min). Variations in the extraction process, the origins of pectin, and factors such as fruit variety and maturity all significantly influence both the quantity and quality of the extracted pectin (Abid et al., 2016; Abid et al., 2017).

3.2. Sugar composition

The monosaccharide composition of PPP and various U-PPPs is presented in Table 1. The results showed that PPP was primarily composed of galacturonic acid (GalU), with notable amounts of glucose (Glu), galactose (Gal), and arabinose (Ara). These results align with previous studies on the monosaccharide profiles of pectin extracted from the peels of different pomegranate cultivars (Abid et al., 2016). However, variations in monosaccharide percentages can be attributed to differences in the raw material's origin, the extraction method employed, and subsequent pectin treatments (Wang et al., 2021). The glucose present likely originates from non-pectic substances such as starch, hemicelluloses, or residual soluble sugars in the peels that were not removed during pectin extraction and processing (Zhang, Ye, Ding, et al., 2013). Additionally, both PPP and U-PPPs revealed the presence of rhamnose (Rha), xylose (Xyl), and trace amounts of mannose (Man) and fucose (Fuc) (Table 1). Pectin structure comprises two regions: homogalacturonan (HG), known as the smooth region, and rhamnogalacturonan (RG-I and RG-II), referred to as the hairy region. Ara and Gal

Table 1
Monosaccharide composition of the pomegranate peel pectin degraded under different ultrasonic treatment times.

Ultrasonic treatment time (min)	type of monosaccharide								
	GalU (%)	Glu (%)	Ara (%)	Gal (%)	Rha (%)	Xyl (%)	Man (%)	Fuc (%)	Rha/GalU
0	64.37 ± 1.60	19.84 ± 4.89	5.49 ± 0.60	5.77 ± 0.69	2.99 ± 0.35	1.04 ± 0.12	0.20 ± 0.05	0.26 ± 0.02	0.03
5	63.24 ± 7.76	19.78 ± 2.49	5.95 ± 0.39	6.15 ± 0.40	3.23 ± 0.21	1.08 ± 0.09	0.25 ± 0.03	0.28 ± 0.01	0.05
10	64.97 ± 3.44	18.58 ± 2.44	5.76 ± 0.34	5.95 ± 0.39	3.13 ± 0.20	1.10 ± 0.12	0.22 ± 0.04	0.25 ± 0.01	0.04
15	65.57 ± 8.42	18.14 ± 1.49	5.82 ± 0.24	5.85 ± 0.30	3.03 ± 0.13	1.06 ± 0.09	0.23 ± 0.03	0.26 ± 0.01	0.04
30	67.16 ± 9.25	17.00 ± 2.51	5.57 ± 0.92	5.70 ± 0.78	3.00 ± 0.41	1.08 ± 0.11	0.21 ± 0.03	0.26 ± 0.05	0.03

originate from the RG-I side chains, while rhamnose is bonded to GalU in the parental chain, forming branching points. Xylose (Xyl) may derive from xylogalactan (Ogutu & Mu, 2017).

The sonication process did not alter the types of monosaccharides present compared with native PPP. The most noticeable change was in the levels of specific sugars in sonicated pectin, which generally exhibited a decrease in Glu content and an increase in GalU content as sonication time increased. However, no statistical differences were observed in the monosaccharide content between PPP and U-PPPs ($P > 0.05$). As expected, GalU remained the predominant monosaccharide residue in all sonicated samples, with its content increasing during sonication (Table 1). This increase might be due to the cleavage of pectin side chains, leading to a higher GalU concentration in the main chain, from 64.37 % *w*/w in PPP to 67.16 % w/w in the U-PPP-30.

A similar trend was observed in citrus pectin during ultrasound processing at various intensities (21.2 and 104.7 W/cm^2) and times (5–60 min), where monosaccharide types remained unchanged. However, the content of GalUA significantly increased with ultrasonication time and intensity as a result of the scission of the side chain of pectin. The greater resistance of GalU compared to neutral sugars explains this increase (Qiu, Cai, et al., 2019).

The Rha/GalU molar ratio is commonly used to indicate the proportion of RG-I regions relative to the HG backbone in pectin structures. In sonicated samples, the relative abundance of HG regions is predominant over RG-I block, as evidenced by the decreased Rha/GalU ratio (Table 1). The minor variation in the Rha/GalUA ratio suggests that power ultrasound, especially at lower ultrasonic intensities, exerted minimal effects on the main chain of pectin (Qiu, Cai, et al., 2019). The reduction of pectin side chains has been reported for apple pectin after ultrasound treatment at 181 and 302 W/cm^2, based on the Rha/GalUA and (Gal + Ara)/Rha ratios (Zhang, Ye, Ding, et al., 2013). In accordance with our results, the HG portion of pectin extracted from unripe raspberry fruit pomaces increased after ultrasonic modification (400 W for 60 min), from 60.14 ± 1.13 % to 66.06 ± 0.30 %, while RG-I was present at lower concentrations compared to the original pectin. Chen et al. (2020) stated that sonication reduced the branching degree of pectin, and sonicated samples were more linear than native pectin.

3.3. Size, ζ-potential, and molecular weight

Table 2 presents the physical characteristics of PPP and U-PPPs, including the droplet size, ζ-potential, and molecular weight under varying ultrasonic durations (0–30 min). The particle size significantly decreased ($P < 0.05$) from 1152.07 ± 45.5 nm to 734.05 ± 8.95 nm as the ultrasonic time increased from 0 to 30 min, representing a 26.30–36.28 % reduction compared to the native PPP. A similar trend was observed in watermelon peel pectin subjected to ultrasonic treatment at 400 W for 5–15 min, which was attributed to the ultrasonic fragmentation of molecules owing to the interparticle collisions and shockwaves produced by the collapse of cavitation bubbles within the pectin solution (Guo et al., 2021).

Notably, the negatively charged ζ-potential of U-PPPs solutions, ranging from −19.15 ± 0.15 mV to −21.3 ± 0.70 mV, was lower than that of PPP (−15.50 ± 1.7 mV) (Table 2). The ζ-potential showed a positive correlation with GalU content and became more negative as the degree of esterification (DE) decreased. This change was likely due to the emergence of a greater number of non-methyl esterified carboxyl groups on the pectin molecules (Wang et al., 2021).

As seen in Table 2, the *Mw* of PPP was 135.6 kDa. It was lower than the values reported by Gavlighi et al. (2018) for pomegranate peel pectin extracted using acid (6385.65 g/ml), enzyme (422.55 g/ml), and buffer (18,631.85 g/ml). Variations in raw materials and extraction conditions likely contributed to these differences. As shown in Table 2, the *Mw* of all U-PPPs was significantly lower than that of PPP ($P < 0.05$). Cavitation induces both mechanical and chemical effects, leading to the degradation of polysaccharides during ultrasound treatment (Zhang, Ye, Ding, et al., 2013). The high shear forces from collapsing cavitation bubbles cause the cleavage of glycosidic bonds in polysaccharides during ultrasonic treatment (Chen et al., 2021). Similarly, the *Mw* of hawthorn pectin (Chen et al., 2019), sweet potato pectin (Ogutu & Mu, 2017), and citrus pectin (Zhang, Ye, Xue, et al., 2013) were reported to decrease significantly with extended sonication time.

However, the ultrasonic frequency and power are crucial factors in determining the cavitation yield and, consequently, the extent of pectin degradation and molecular weight reduction in different studies (Chen et al., 2021).The *Mw* of PPP decreased significantly from 125.4 to 59.95 kDa with sonication times ranging from 5 to 15 min ($P < 0.05$), but it increased to 92.6 kDa at 30 min. A similar increase in the molecular weight of citrus pectin was observed with prolonged sonication time (more than 30 min) at 302 W/cm^2. This finding indicates that hydrodynamic forces primarily affect the cleavage of longer polysaccharide chains, whereas chains below a certain critical size may remain unaffected (Zhang, Ye, Xue, et al., 2013).

The polydispersity index (*Mw*/Mn) can be used to assess the differences in the molecular weight distributions of PPP and U-PPPs. The PPP exhibited a narrower molecular mass distribution compared to U-PPPs (Table 2). The polydispersity index of U-PPPs did not display a consistent trend with increasing sonication time, suggesting a random fracture

Table 2
Particle size, ζ-potential, molecular weight, and degree of esterification of the pomegranate peel pectin degraded under different ultrasonic treatment times.

Ultrasonic treatment time (min)	Particle size (nm)	ζ-potential (mv)	Molecular weight (kD)	Mn (kDa)	Mw/Mn	Degree of esterification (%)
0	1152.07 ± 45.50 a	15.50 ± 1.70 c	135.60 ± 5.51 a	97.45 ± 2.67 a	1.39	61.7 ± 1.99 a
5	849.00 ± 2.00 b	19.15 ± 0.15 b	125.40 ± 4.66 b	88.10 ± 1.63 b	1.42	56.52 ± 0.19 b
10	831.50 ± 21.50 b	19.95 ± 0.35 ab	116.65 ± 4.73 c	53.20 ± 6.08 c	2.19	52.8 ± 1.43 bc
15	807.50 ± 3.50 b	20.50 ± 0.00 ab	59.95 ± 0.77 e	38.05 ± 1.20 d	1.57	50.53 ± 0.80 cd
30	734.05 ± 8.95 c	21.30 ± 0.70 a	92.60 ± 0.56 d	32.60 ± 3.67 e	2.84	47.89 ± 2.08 d

Values are mean ± standard deviation (n = 3). For each attribute, values with the different lowercase letters are significantly different ($P < 0.05$).

of the PPP chain and the generation of the broad range of polymer size distributions. A similar phenomenon was previously described for sweet potato pectin in the sonolyzed at 200 W for 5–20 min (Ogutu & Mu, 2017).

3.4. Degree of esterification

The degree of esterification (DE) is a critical parameter that influences the applicability and functionality of pectin, including its emulsifying capacity and gelling properties. The DE value of PPP was found to be 61.7 ± 1.99 % (Table 2), indicating that the PPP can be classified as highly methylated pectin. DE value of 67.17 % has been reported for pectin extracted from pomegranate peel using HCl solution (pH = 1.5) (Sharifi et al., 2022). Several factors, including plant variety, maturity level, and extraction techniques, impact the quality of extracted pectin (Abid et al., 2016).

The DE values of U-PPPs were significantly reduced ($P < 0.05$) by ultrasonic modification (Table 2), with a greater reduction observed at extended sonication times. For instance, modification of hawthorn pectin at 20 kHz, with a power of 130 W and duty cycle of 3 on/5 s off, led to a significant reduction in DE values from 25.5 % in raw pectin to 13.88 % after 10 min of sonication (Chen et al., 2019). The reduction in DE likely resulted from the hydrolysis of ester bonds due to acoustic cavitation or the reaction between ester groups and reactive species generated during sonolysis (Ogutu & Mu, 2017). The decreased DE of the pectin molecules led to a reduction in steric hindrances, increasing the flexibility of the pectin chains and promoting further degradation through the cavitation effect (Qiu, Cai, et al., 2019). U-PPP-30 exhibited DE values below 50 % after sonication, indicating its potential as a gelling agent in low-sugar product formulations.

3.5. FTIR analysis

FTIR spectroscopy was employed to evaluate the structural changes in PPP resulting from ultrasonication (Fig. 1). All samples exhibited the major characteristic absorption peaks of pectin. For PPP, a strong and broad absorption peak at approximately 3307 cm^{-1} was associated with the stretching vibration of O—H groups, indicative of the intra- and inter-molecular hydrogen bonds within the GalU unit in the pectin backbone. However, a notable reduction in absorption peak intensity and a shift to a higher wavenumber (3307 → 3341 cm^{-1}) were observed with increasing ultrasonication time for PPHs. This shift was likely due to intensified molecular motion associated with the super-mixing effect of ultrasonication (Guo et al., 2021).

The peak observed in the range of 2936 to 2931 cm^{-1} corresponded to the C—H stretching of alkane groups (-CH_3, -CH_2, -CH). Similar bands have been reported in the FTIR spectra of pectin extracted from pomegranate peel (Abid et al., 2017; Yang et al., 2018). The absorption peak in the range of 1725 to 1727 cm^{-1} was attributed to the C═O stretching vibration of methyl-esterified carboxyl groups ($COOCH_3$), while the absorption at 1618 to 1620 cm^{-1} was related to C═O stretching vibration of ionic carboxyl groups (COO-). These peaks provide valuable information regarding the DE of pectin. The FTIR spectrum of PPP displayed higher absorbance around 1725 cm^{-1} ($COOCH_3$) compared to 1620 cm^{-1} (COO-), indicating high methoxyl PPP (Fig. 1). As the ultrasonic time increased from 5 to 30 min, the absorption peak around 1618 cm^{-1} was enhanced, while the intensity of the peak around 1725 cm^{-1} decreased. These changes in the FTIR spectra corroborate the increased GalU content and decreasing trend in DE values of U-PPPs, as determined by the titration method.

Carboxyl groups also exhibited bending vibration of C-OH at 1440–1441 cm^{-1} and the flexural vibration of the hydroxyl (-OH) group of alcohol at 1328 cm^{-1} (Chen et al., 2019; Sharifi et al., 2022). The spectral range below 1500 cm^{-1} is a characteristic region for polysaccharides, corresponding principally to the C–O–C, C—C, and C–OH mode of glycosidic linkage and sugar ring vibrations (Abid et al., 2017; Ogutu & Mu, 2017). The absorption peaks at approximately 951 and 889 cm^{-1} were assigned to *β-D-* glucopyranosyl and *β-D-*mannose, respectively (Qiu, Zhang, & Wang, 2019; Zhang, Ye, Ding, et al., 2013). Our findings suggested that, although ultrasound treatment is accompanied by the degradation of the PPP side chains, the primary structure of pectin remains unchanged. There have been no significant changes observed in the main chain of sweet potato pectin following sonication for durations of 5, 10, and 20 min (Ogutu & Mu, 2017).

3.6. Turbidity and color attributes

The color and turbidity of the pectin solution are key factors that play a significant role in the optical properties of the final product and consumer acceptance. As shown in Table 3, the PPP solution (0.5 %) was

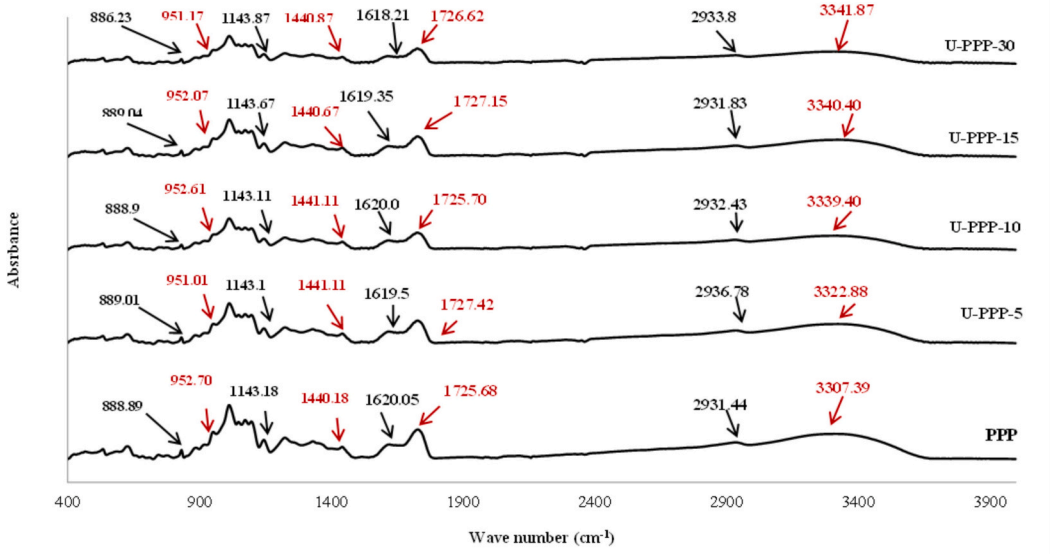

Fig. 1. FTIR spectra of pomegranate peel pectin under different ultrasonic treatment times. PPP: Pomegranate peel pectin, U-PPP-5: PPP sonicated for 5 min, U-PPP-10: PPP sonicated for 10 min, U-PPP-15: PPP sonicated for 15 min, U-PPP-30: PPP sonicated for 30 min.

Table 3
Turbidity and color attributes (L^*, a^*, b^* and ΔE) of the solutions (5 mg/ml) of pomegranate peel pectin degraded under different ultrasonic treatment times.

Ultrasonic treatment time (min)	Turbidity	L^*	a^*	b^*	ΔE
0	0.40 ± 0.002 a	58.17 ± 0.05 e	4.23 ± 0.04 a	16.15 ± 0.05 a	–
5	0.39 ± 0.001 a	61.24 ± 0.04 d	3.46 ± 0.03 b	15.80 ± 0.07 b	3.18 ± 0.03 d
10	0.38 ± 0.002 a	63.09 ± 0.04 c	3.19 ± 0.04 c	14.33 ± 0.01 c	5.34 ± 0.02 c
15	0.36 ± 0.001 b	65.51 ± 0.19 b	2.99 ± 0.08 d	14.06 ± 0.03 d	7.73 ± 0.09 b
30	0.23 ± 0.002 c	66.20 ± 0.15 a	2.85 ± 0.05 e	13.89 ± 0.01 e	8.45 ± 0.08 a

Values are mean ± standard deviation (n = 3). For each attribute, values with the different lowercase letters are significantly different ($P < 0.05$).

significantly more turbid than the U-PPP solutions ($P < 0.05$), as indicated by the higher absorbance at 480 nm. U-PPP-30 exhibited the highest brightness, followed by U-PPP-15. The hawthorn pectin solution (5 mg/ml) showed a notable reduction in OD_{480}, decreasing from 0.346 in raw pectin solution to 0.237–0.297 in sonicated samples treated for 0.5–10 min at 130 W (Chen et al., 2019). Seshadri et al. (2003) reported that gels obtained from ultrasonically pretreated apple pectin (40 W, 5–60 min) were significantly less turbid than those made from raw pectin, likely due to the degradation of the pectin chain, the release of polyphenols from the structure, and an increase in light scattering.

The Hunter Lab color values of the samples are presented in Table 3. During extraction, the disintegration of the cell wall allowed pigments or polyphenols trapped in the pectin to impart a yellow-orange color to the PPP solution. Sharifi et al. (2022) reported different L^* (55.05), a^* (−0.68), and b^* (15.27) values for pomegranate pectin extracted by the conventional methods, which could be attributed to the differences in the color components of the raw materials and the extraction method. As ultrasonication time increased, the L^* value increased significantly, while the b^* and a^* values showed a decreasing trend. This may be due to ultrasonic treatment, which loosens weak bonds between pectin and extracted coloring pigments, followed by the breakdown of pigments into colorless fragments (Gharibzahedi et al., 2019; Sharifi et al., 2022).

ΔE quantifies the color variation between PPP and U-PPP samples. As seen in Table 3, the ΔE values of U-PPP solutions varied between 3.18 and 3.45. U-PPP-30 presented the highest ΔE value compared to PPP. The perception of color differences (ΔE) changed based on the color observed and the sensitivity of the human eye: $\Delta E < 1$: the differences are indistinguishable to the human eye; $1 < \Delta E < 3$: the differences are minor but detectable; and $\Delta E > 3$, the differences are clearly noticeable by the human eye (Bodart et al., 2008). Therefore, the differences observed instrumentally between PPP and U-PPP samples could also be detected by human eyes. No study on the effect of ultrasound-assisted depolymerization on the color attributes of pectin solution was found. However, pectin extracted from fig skin using an ultrasound-microwave-assisted method exhibited a lighter appearance, with lower b^* and a^* values, compared to pectin extracted using acidic hot water (Gharibzahedi et al., 2019). Since pectin's color is considered a critical quality factor for its application in food and pharmaceutical formulations, ultrasound can be considered as a technique for modifying its color properties.

3.7. Total phenolic content and antioxidant activity

The TPC of PPP was measured at 30.67 ± 1.46 mg GAE/g pectin (Fig. 2A), consistent with the substantial amounts (204 ± 0.2 mg GAE/g) of phenolic compounds present in pomegranate peel (Mirab et al., 2020). The TPC of PPP was lower than that reported for pectin extracted from sour orange peel (39.95 mg GAE/g) (Hosseini et al., 2019). It is well-known that the TPC of extracted pectin is influenced by various factors, including the raw material, extraction method, polyphenol structure, and structural characteristics of pectin, such as DE and branching ratio (Hosseini et al., 2019; Liu et al., 2020).

Under the ultrasonic modification, the TPC significantly increased ($P < 0.05$) in U-PPPs compared to PPP, reaching 34.49–41.38 mg GAE/g pectin. The trend is comparable to findings from earlier studies, where the TPC of unripe raspberry pomace pectin increased from 49.06 to 74.19 mg GAE/g pectin after 60 min ultrasonication at 400 w (2 s on/2 s off). This increase might be due to the altered polyphenol binding capacity resulting from the chemical and conformational modifications of the pectin structure induced by ultrasonic treatment (Chen et al., 2020). Additionally, the collapse of cavitation bubbles promotes the disintegration of matrix constituents, facilitating deeper solvent penetration into the material and thus releasing more polyphenols into the solvent (Nag & Sit, 2018).

Fig. 2B illustrates the DPPH scavenging activity of PPP and U-PPPs as a function of concentration (25–250 μg/ml). PPP exhibited significant DPPH scavenging activity with a dose-dependent pattern (51.71–77.85 %). Ultrasonication enhanced the scavenging activity of PPP, with a more pronounced effect observed in U-PPP-10, U-PPP-15, and U-PPP-30, where the scavenging activity ranged from 62.53 to 84.13 %, 62.90–82.87 %, and 60.31–84.75 %, respectively, within the studied concentration range.

The FRAP of PPP was significantly lower than those of U-PPPs at all investigated concentrations ($P < 0.05$) (Fig. 2C). Furthermore, all samples demonstrated a notable increase in FRAP as the concentration increased ($P < 0.05$), with the highest FRAP activity observed at 1000 μg/l. No significant differences in FRAP were noted among U-PPP-10, U-PPP-15, and U-PPP-30 at concentrations of 250 and 500 μg/l ($P > 0.05$). The highest FRAP was recorded for U-PPP-30, exhibiting values between 3.29 and 4.01 μM Fe^{2+}/mg sample at concentrations of 500–1000 μg/ml, respectively. The FRAP activity of pectin extracted from the slimy sheath of jackfruit seeds was 10.4 ± 0.51 μM, which was higher than that of commercial citrus and apple pectins, with values of 4.21 ± 0.6 μM and 5.96 ± 0.19 μM, respectively. This finding was attributed to the phenolic compounds co-extracted with the pectin (Kumar et al., 2021).

The phenolic compounds present in the samples contribute, to some extent, to the FRAP and radical scavenging of PPP and U-PPPs (Chen et al., 2020; Kumar et al., 2021). The antioxidant activity can also be attributed to the presence of various hydroxyl and carboxyl groups in their monosaccharide units, particularly in GalU, which serve as electron donors. Moreover, pectin may terminate free radical chain reactions by binding radical ions to form more stable compounds (Gharibzahedi et al., 2019).

Native pectin is characterized by a complex side groups structure. During sonication treatment, the large molecule undergoes depolymerization, resulting in pectin with a lower *Mw*. This process exposes previously hidden groups and generates new functional carbonyl groups at the scission sites (Ogutu & Mu, 2017). Ultrasonication increased the GalU content, which was accompanied by an abundance of free carboxyl groups in the structure of sonicated samples, leading to an increase in the antioxidant activity. Qiu, Zhang, and Wang (2019) also observed that prolonged exposure of *Auricularia auricula* polysaccharides to ultrasound (500 w for 2–12 h) resulted in decreased molecular weight, viscosity, and chain length while increasing the availability of O—H groups and, thereby enhancing ABTS radical scavenging ability.

3.8. α- amylase inhibition activity

Polysaccharide-based α-amylase and/or α-glucosidase inhibitors have recently garnered significant interest as oral hypoglycaemic agents

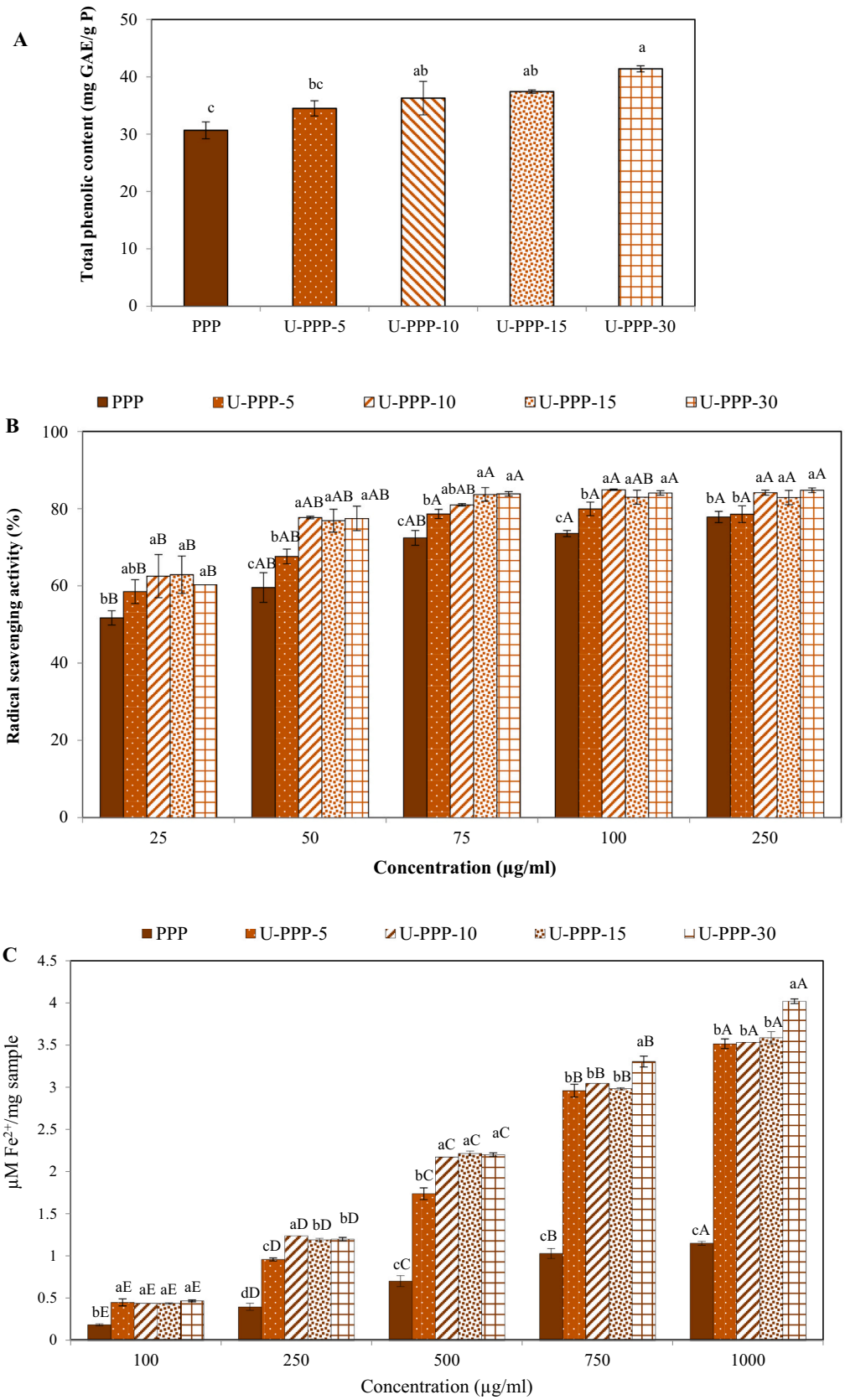

Fig. 2. Effect of ultrasonic treatment time on total phenolic content (mg GAE/g) (A) and DPPH radical scavenging activity (%) (B), and Ferric-reducing antioxidant power (µM Fe^{2+}/mg) (C) of pomegranate peel pectin.
The data are the mean ± standard deviation ($n = 3$). In Fig. 2A values with different lowercase letters on the bars are significantly different ($P < 0.05$). In Fig. 2 B&C, different lowercase letters show significant differences ($P < 0.05$) between the samples at the same concentration, and different uppercase letters indicate significant differences ($P < 0.05$) between the different concentrations of each sample. PPP: Pomegranate peel pectin, U-PPP-5: PPP sonicated for 5 min, U-PPP-10: PPP sonicated for 10 min, U-PPP-15: PPP sonicated for 15 min, U-PPP-30: PPP sonicated for 30 min.

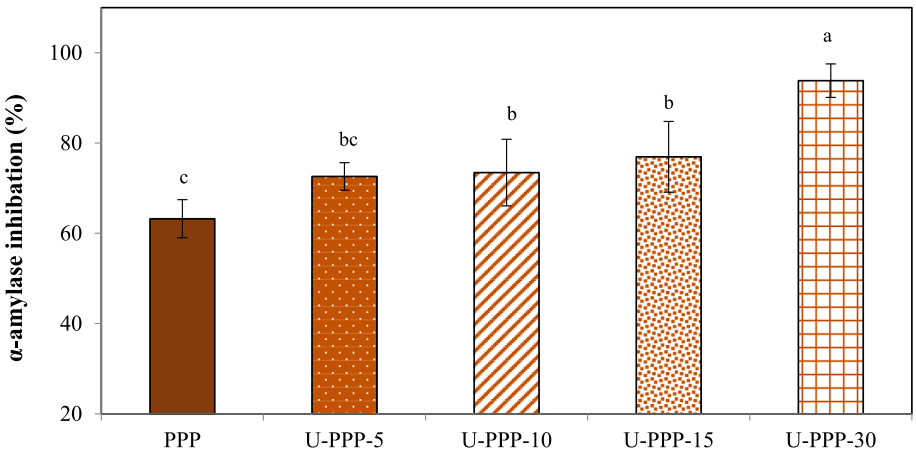

Fig. 3. Effect of ultrasonic treatment time on the α-amylase inhibitory activity (%) of pomegranate peel pectin at a concentration of 10 mg/ml.
The data are the mean ± standard deviation ($n = 3$). Values with different lowercase letters on the bars are significantly different ($P < 0.05$). PPP: Pomegranate peel pectin, U-PPP-5: PPP sonicated for 5 min, U-PPP-10: PPP sonicated for 10 min, U-PPP-15: PPP sonicated for 15 min, U-PPP-30: PPP sonicated for 30 min.

for diabetics due to their ability to delay postprandial rise in blood glucose levels (Xu et al., 2018). In this study, PPP exhibited a notable α-amylase inhibitory activity of 63.23 ± 4.22 % at the tested concentration, with ultrasonication further enhancing this inhibitory effect (Fig. 3). As expected, the α-amylase inhibitory activity of PPP and U-PPPs was lower than that of acarbose (used as a positive control) with an IC_{50} of 125 μg/ml, which is likely due to the pure nature of the synthetic inhibitor.

Previous studies have reported contradictory findings regarding the α-amylase inhibition activity of pectin. Pectin from various sources may reduce, enhance, or have no effect on the rate and/or extent of α-amylase activity. However, in vitro α-amylase inhibition by pectin is generally attributed to two possible mechanisms: (i) the inhibition of starch access to α-amylase by increasing digesta viscosity, and (ii) direct interaction with α-amylase, impacting starch hydrolysis (Bai et al., 2021). In line with our results, a pectin-like polysaccharide extracted from *Momordica charantia exhibited significant α-amylase inhibition, with an effect of* 89.1 % at a concentration of 10 mg/ml (Tan & Gan, 2016). The variations observed across studies may be partly attributed to differences in experimental conditions (e.g., pH, pectin concentration, the concentration of multivalent cations) and pectin characteristics (e.g., structure, solubility, and gelation conditions) (Bai et al., 2021).

Among the ultrasonicated pectin samples, U-PPP-30, which underwent the longest duration of ultrasonic treatment, exhibited the highest α-amylase inhibition activities (93.82 ± 3.7 %). The inhibition rates for U-PPP-5, U-PPP-10, and U-PPP-15 were 72.60 ± 3.04, 73.45 ± 7.39, and 76.96 ± 7.84 %, respectively. According to Bai et al. (2021), pectins with a lower DE exhibit stronger inhibitory effects on α-amylase activity. Additionally, the degradation of raspberry fruit polysaccharides by Fe^{2+}-H_2O_2 treatment increased the α-amylase inhibition from 38.81 ±

Table 4
Changes in pH, titratable acidity (%), and populations of *L. casei* and *B. longum* (log CFU/ml) in glucose-free MRSB medium contain pomegranate peel pectin, ultrasonic-treated pomegranate peel pectin for 30 min, and inulin during 48 h fermentation.

Properties	Prebiotic type	*L. casei*			*B. longum*		
		0	24	48	0	24	48
Probiotic count (Log CFU/ml)	Control negative	4.47 ± 0.00 abB	5.72 ± 0.110 eA	5.67 ± 0.010 dA	4.44 ± 0.030 abB	5.56 ± 0.000 eA	5.62 ± 0.035 fA
	Glucose (2 %)	4.52 ± 0.057 abB	9.46 ± 0.106 aA	9.17 ± 0.240 bA	4.37 ± 0.125 abB	9.64 ± 0.100 aA	9.21 ± 0.046 bA
	PPP-0.5 %	4.57 ± 0.052 abC	6.52 ± 0.0260 dB	7.48 ± 0.062 cA	4.48 ± 0.051 aC	6.81 ± 0.049 dB	7.71 ± 0.096 eA
	PPP-1 %	4.86 ± 0.051 aC	6.86 ± 0.018 dB	7.71 ± 0.018 cA	4.25 ± 0.002 bC	6.98 ± 0.083 dB	8.02 ± 0.118 dA
	U-PPP-30-0.5 %	4.53 ± 0.051 abC	8.57 ± 0.066 bcB	9.01 ± 0.054 bA	4.42 ± 0.081 abB	8.95 ± 0.018 bA	9.18 ± 0.057 bA
	U-PPP-30-1 %	4.43 ± 0.007 abC	8.97 ± 0.043 bB	9.69 ± 0.088 aA	4.23 ± 0.092 bC	9.06 ± 0.009 bB	9.86 ± 0.041 aA
	Inulin-0.5 %	4.19 ± 0.014 bC	8.08 ± 0.069 cB	9.03 ± 0.070 bA	4.33 ± 0.049 abC	7.99 ± 0.043 cB	8.69 ± 0.077 cA
	Inulin-1 %	4.24 ± 0.036 abC	8.69 ± 0.082 cB	9.38 ± 0.004 abA	4.21 ± 0.110 bB	8.40 ± 0.041 cA	8.87 ± 0.008 cA
pH	Control negative	6.39 ± 0.009 aB	6.87 ± 0.008 aA	6.82 ± 0.010 aA	6.38 ± 0.014 aC	6.95 ± 0.016 aA	6.85 ± 0.012 aB
	Glucose (2 %)	6.17 ± 0.009 bA	4.41 ± 0.000 hB	4.18 ± 0.010 fC	6.23 ± 0.010 bA	4.36 ± 0.030 gB	4.12 ± 0.030 gC
	PPP-0.5 %	6.12 ± 0.018 bA	5.93 ± 0.000 cB	5.81 ± 0.009 bC	6.11 ± 0.012 cA	5.88 ± 0.032 cB	5.69 ± 0.028 cC
	PPP-1 %	5.99 ± 0.042 cdA	5.78 ± 0.020 dB	5.63 ± 0.016 cC	5.99 ± 0.016 dA	5.70 ± 0.028 dB	5.48 ± 0.000 dC
	U-PPP-30-0.5 %	6.05 ± 0.004 cA	5.42 ± 0.004 eB	5.41 ± 0.012 dB	6.06 ± 0.000 cdA	5.44 ± 0.020 eB	5.37 ± 0.010 eB
	U-PPP-30-1 %	5.97 ± 0.030 dA	5.17 ± 0.016 gB	5.05 ± 0.009 eC	5.92 ± 0.010 dA	5.15 ± 0.000 fB	5.10 ± 0.012 fB
	Inulin-0.5 %	6.34 ± 0.016 aA	5.97 ± 0.014 bB	5.76 ± 0.012 bC	6.30 ± 0.012 abA	5.96 ± 0.028 bB	5.93 ± 0.010 bB
	Inulin-1 %	6.37 ± 0.010 aA	5.82 ± 0.010 dB	5.58 ± 0.000 cC	6.32 ± 0.010 aA	5.94 ± 0.010 bcB	5.75 ± 0.040 cC
Acidity (% lactic acid)	Control -	0.33 ± 0.022 cA	0.312 ± 0.008 dA	0.31 ± 0.016 eA	0.33 ± 0.016 bA	0.30 ± 0.008 eA	0.32 ± 0.008 eA
	Glucose (2 %)	0.37 ± 0.008 abcC	2.43 ± 0.084 aB	2.79 ± 0.044 aA	0.37 ± 0.008 abC	2.48 ± 0.092 aB	2.95 ± 0.092 aA
	PPP-0.5 %	0.39 ± 0.016 abcC	0.51 ± 0.014 cB	0.56 ± 0.016 dA	0.39 ± 0.014 abB	0.53 ± 0.022 dB	0.55 ± 0.008 cdA
	PPP-1 %	0.42 ± 0.008 abcC	0.58 ± 0.008 cB	0.59 ± 0.025 dA	0.44 ± 0.008 aC	0.57 ± 0.008 dB	0.58 ± 0.008 cdA
	U-PPP-30-0.5 %	0.45 ± 0.008 abB	0.67 ± 0.008 bA	0.75 ± 0.008 cA	0.42 ± 0.008 abB	0.65 ± 0.008 cA	0.72 ± 0.008 cA
	U-PPP-30-1 %	0.46 ± 0.008 aC	0.74 ± 0.008 bB	0.87 ± 0.014 bA	0.44 ± 0.000 aB	0.75 ± 0.008 bA	0.84 ± 0.008 bA
	Inulin-0.5 %	0.36 ± 0.019 cC	0.48 ± 0.042 cB	0.59 ± 0.014 dA	0.35 ± 0.022 abC	0.45 ± 0.014 dB	0.49 ± 0.008 dA
	Inulin-1 %	0.36 ± 0.014 cC	0.51 ± 0.008 cB	0.64 ± 0.008 dA	0.34 ± 0.014 bC	0.58 ± 0.220 dB	0.58 ± 0.014 cdA

Values are mean ± standard deviation (n = 3). For each strain and parameter, at the same time, values in the same column with the different lowercase letters are significantly different ($P < 0.05$). For each strain, and parameter, and same prebiotic, values in the same row with the different uppercase letters are significantly different ($P < 0.05$). PPP: pomegranate peel pectin, U-PPP-30: ultrasonic-treated pomegranate peel pectin for 30 min.

1.68 % in raw polysaccharides to 49.94 ± 1.14 % in degraded polysaccharides at a concentration of 4.0 mg/ml. High molecular weight may affect the binding capacity of polysaccharides to the active site of digestive enzymes. However, further structural characterization of pectins is necessary to gain a deeper understanding of how pectins affect starch digestion (Xu et al., 2018).

Moreover, Mirab et al. (2020) indicated that pomegranate peel polyphenols could moderately inhibit α-amylase activity. Therefore, the increased α-amylase inhibition observed in U-PPPs can be partially attributed to the increase in TPC and the reduction in DE during ultrasonic treatment. The α-glucosidase inhibition activity of pectin extracted from unripe raspberry fruit pomace was enhanced after ultrasound modification at 400 W for 60 min. Both raw and sonicated samples displayed a concentration-dependent manner with IC_{50} of 0.17 and 0.14 mg/ml, respectively. This enhancement is closely associated with its polyphenol content and the alterations in the functional groups of pectin during irradiation (Chen et al., 2020). Ultrasound-degraded polysaccharides from blackcurrant fruit (treated at 400 and 600 W, for 30 min) exhibited superior α-amylase inhibitory activities compared to intact polysaccharides (Xu et al., 2018).

3.9. Prebiotic activity

Changes in the populations of L. *casei* and *B. longum* following 48 h of in vitro fermentation with PPP, U-PPP-30, glucose, and inulin are shown in Table 4. According to Huebner et al. (2008), the prebiotic activity of carbohydrate substrates refers to their capacity to selectively promote the proliferation of particular probiotic strains relative to non-prebiotic substances such as glucose. Initial L. *casei* and *B. longum* counts were between 4.17 and 4.86 and 4.21–4.48 Log CFU/ml at t_0, respectively. All substrates stimulated the growth of L. *casei* during the 24-h fermentation period. The increase in L. *casei* cell count for the negative control (1.25 Log_{10} CFU/ml), PPP-0.5 % (1.95 Log_{10} CFU/ml), PPP-1 (2 Log_{10} CFU/ml), inulin-0.5 % (3.98 Log_{10}CFU/ml), was significantly lower than that observed with glucose (4.94 Log_{10} CFU/ml). However, the values for U-PPP-30-0.5 % (4.22 Log_{10} CFU/ml), U-PPP-30-1 % (4.54 Log_{10} CFU/ml), and inulin-1 % (4.45 Log_{10} CFU/ml) were comparable to glucose. Although U-PPP-30-1 % promoted significantly higher ($P < 0.05$) *L. casei* proliferation among all substrates tested at t_{48}, no significant differences were found between inulin-0.5 %, inulin-1 %, glucose, and U-PPP-30-0.5 % (Table 4).

The results also demonstrated that *B. longum* exhibited selectivity in assimilating individual substrates during the initial 24 h of fermentation, following the order: glucose > U-PPP-30-1 % > U-PPP-30-0.5 % > inulin-1 % and inulin-0.5 % > PPP-1 % > PPP-0.5 %. At the end of fermentation, the population of *B. longum* reached 7.71–8.02, 9.18–9.86, and 8.69–8.87 Log_{10} CFU/ml in GF-MRSB supplemented with different concentrations of PPP, U-PPP-30, and inulin, respectively. Although PPP gradually stimulated the growth of both probiotics throughout the fermentation, the counts of L. *casei* or *B. longum* on this substrate were notably lower than those observed with U-PPP-30 and inulin at the same concentration. A dose-response relationship was noted between the concentrations of U-PPP-30 or PPP and the growth of *B. longum* at t_{48}. Our results revealed that U-PPP-30 supported similar growth of both strains relative to glucose throughout the 48-h incubation period.

The acidifying activity of L. *casei* and *B. longum* was further assessed by measuring changes in the pH and TA of SF-MRSB media, with results presented in Table 4. The rise in bacterial populations in the presence of prebiotics coincided with a decline in pH and an increase in acidity values. At t_{24}, glucose-supplemented SF-MRSB exhibited the most significant decrease in pH and the greatest increase in TA for both strains (Table 4). This can be attributed to the high availability of easily accessible sugars utilized by L. *casei* and *B. longum.* The TA of the positive control increased over time, from 0.375 % at t_0 to 2.43 % and 2.48 % at t_{24}, with L. *casei* and *B. longum*, respectively, further rising to 2.79 % and 2.95 % at t_{48}.

Pectins are known as highly fermentable dietary fibers. Several studies have documented the prebiotic potential of pectin polysaccharides derived from agriculture byproducts, including pistachio peel (Akbari-Alavijeh et al., 2018) and citrus peel (Zhang et al., 2018). Results demonstrated that U-PPP-30 promoted higher growth of L. *casei* and *B. longum* compared to PPP. Structural characteristics such as molecular weight, sugar composition, esterification degree, and branching degree may influence the accessibility of pectin and POSs to probiotics (Zhu et al., 2019). Previous studies have indicated a strong association between the molecular weight of pectin and its prebiotic activity. POSs obtained from okra pectin by Fenton reaction promoted higher growth of L. *rhamnosus* and *B. longum* compared to raw pectin, owing in part to their lower molecular weight and shorter chain length (Yeung et al., 2021). The enzymatic modification of citrus pectin enhanced the growth and acid tolerance of *B. bifidum* and L. *acidophilus* by providing readily available monosaccharides (Ho et al., 2017).

The metabolism of PPP, U-PPP-30, and inulin resulted in a gradual decrease in the pH of SF-MRSB, indicating that *B. longum* and *L.casei* were able to metabolize these substrates. For L. *casei*, the glucose-supplemented sample exhibited a decrease of 1.76 pH unit at t_{24}, followed by U-PPP-30-1 %, U-PPP-30-0.5 %, inulin-1 %, inulin-0.5 %, PPP-1 %, and PPP-0.5 %, with reductions of 0.8, 0.63, 0.55, 0.37, 0.21, and 0.19 pH units, respectively. Except for the negative control and PPH-30-0.5 % samples, significant pH declines were observed for other samples during the second day of fermentation with L. *casei.* The TA of samples containing inulin, PPP, and U-PPP-30 increased by 60.97–78.33 %, 39.43–44.61 %, and 65.78–85.89 % during 48 h of fermentation by L. *casei*, respectively.

Regarding *B. longum,* the culture medium with glucose exhibited the highest pH drop at t_{24} (1.87 unit), followed by the U-PPP-30-1 % and U-PPP-30-0.5 %, with pH drops of 0.77 and 0.62 units, respectively. The inulin-containing samples showed a pH drop ranging from 0.3 to 0.38 units at t_{24}, noticeably higher than the pH decrease observed in the PPP samples, which ranged from 0.2 to 0.29 units. At t_{48}, the pH values of the glucose, inulin-1 %, PPP-0.5 %, and PPP-1 % samples significantly decreased by 0.24, 0.19, 0.19, and 0.22 units, respectively ($P < 0.05$), while in other samples the pH drop was negligible ($P > 0.05$). After 48 h of fermentation with *B. longum*, the greatest increase in TA values was observed in the following order: PPH-30-1 % (90.5 %) > PPH-30-0.5 % (72.85 %) > inulin-1 % (71.9 %) > PPP-0.5 % (40.9 %) > inulin-0.5 % (39 %) > PPP-1 % (32.3 %). The differences in pH and TA changes could be associated with the distinct metabolic pathways responsible for metabolizing each prebiotic substrate. Probiotics secrete enzymes that hydrolyze polysaccharides like PPP and U-PPP-30 into simple sugar, which are then degraded into short-chain fatty acids (SCFAs) like propionic acid, acetic acid, lactic acid, and butyric acid, leading to a pH decrease in the fermented broth (Akbari-Alavijeh et al., 2018). Extending the hydrolysis time and increasing the concentrations of citrus pectin hydrolysates effectively promoted the growth of *B. bifidum* and *L. acidophilus*, resulting in a greater decrease in pH and higher acid production in the culture medium compared to commercial prebiotics (Ho et al., 2017).

Prebiotic activity scores (PAS) of PPP, U-PPP-30, inulin, for L. *casei* and *B. longum* were derived from the probiotic population of each strain and enteric *E. coli* through the use of Eq. 4. The positive PAS observed with respect to *E. coli* ATCC 25922 indicated that L. *casei* and *B. longum* selectively metabolized all tested prebiotic. As shown in Fig. 4, inulin exhibited the highest efficacy in promoting the growth of both probiotic strains with values of 0.67 for *L. casei* and 0.56 for *B. longum,* followed by U-PPP-30-1 % (0.45 for *L. casei* and 0.47 for *B. longum*), and PPP (0.03 for *L. casei* and 0.05 for *B. longum*). Bifidobacterial genomes encode numerous carbohydrate-modifying enzymes, reflecting their adaptation to a carbohydrate-rich gut environment. The presence or absence of specific hydrolysis and transport systems in bacteria may explain the variations in prebiotic scores (Zhang et al., 2018).

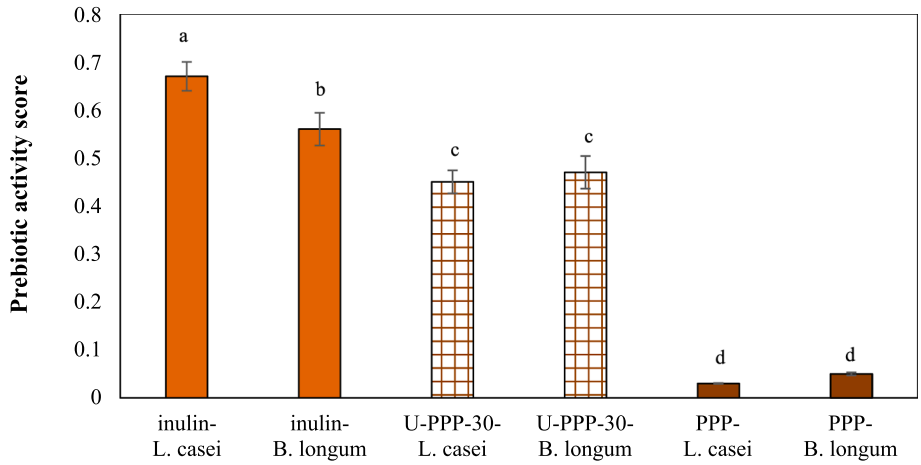

Fig. 4. Prebiotic activity score of pomegranate peel pectin (PPP), pomegranate peel pectin sonicated for 30 min (U-PPP-30), and inulin at a concentration of 1 % (*w/v*) for *B. longum* (ATCC 55813) and L. *casei* (ATCC 393).
The data are the mean ± standard deviation ($n = 3$). Values with different lowercase letters on the bars are significantly different ($P < 0.05$).

4. Conclusion

In this study, pectin from pomegranate peels was degraded using an ultrasound-assisted method. Sonication treatment significantly reduced the *Mw* of pectin. Cavitation phenomena induce mechanical and chemical effects that degrade polysaccharides by cleaving glycosidic bonds through high shear forces from collapsing cavitation bubbles. The reduction in DE likely resulted from the hydrolysis of ester bonds due to acoustic cavitation or reactions with reactive species produced during sonolysis. However, the primary structure of U-PPPs remained similar to that of PPP, as revealed by FTIR analysis. Prolonged sonication contributed to an increase in TPC, thereby enhancing both antioxidant and α-amylase inhibition properties. Consequently, U-PPPs may be considered effective antioxidants and potential antidiabetic agents. Although both PPP and U-PPP-30 were fermentable by the tested probiotics, U-PPP-30 demonstrated a more pronounced stimulatory effect on probiotic proliferation. Additionally, the TA resulting from its fermentation was higher than that observed with inulin and PPP. The PAS of U-PPP-30 was positive and comparable to inulin, suggesting its potential as a valuable component in the development of nutraceuticals and synbiotic foods. In conclusion, sonication treatment can be considered an effective, safe, and environmentally friendly technique for modifying the properties of pectin and enhancing its biological and health-promoting functions. Further research is needed to explore the detailed structure-activity relationship of PPP and U-PPPs.

CRediT authorship contribution statement

Sahar Bachari: Visualization, Methodology, Investigation, Data curation. **Maryam Ghaderi-Ghahfarokhi:** Writing – review & editing, Writing – original draft, Visualization, Validation, Supervision, Software, Resources, Project administration, Methodology, Funding acquisition, Formal analysis, Data curation, Conceptualization. **Hassan Ahmadi Gavlighi:** Methodology, Investigation, Data curation, Conceptualization. **Mehdi Zarei:** Methodology, Investigation, Data curation.

Declaration of competing interest

The authors declare that they have no known competing financial interests or personal relationships that could have appeared to influence the work reported in this paper.

Data availability

No data was used for the research described in the article.

Acknowledgments

This work was supported by the Research Council of Shahid Chamran University of Ahvaz (Grant No: SCU.VF1400.38687). The authors would like to appreciate the valuable assistance of Dr. Mehdi Tabarsa for his cooperation and support in the HPSEC investigation.

References

Abid, M., Cheikhrouhou, S., Renard, C. M., Bureau, S., Cuvelier, G., Attia, H., & Ayadi, M. (2017). Characterization of pectins extracted from pomegranate peel and their gelling properties. *Food Chemistry, 215*, 318–325. https://doi.org/10.1016/j.foodchem.2016.07.181

Abid, M., Renard, C. M., Watrelot, A. A., Fendri, I., Attia, H., & Ayadi, M. (2016). Yield and composition of pectin extracted from Tunisian pomegranate peel. *International Journal of Biological Macromolecules, 93*, 186–194. https://doi.org/10.1016/j.ijbiomac.2016.08.033

Akbari-Alavijeh, S., Soleimanian-Zad, S., Sheikh-Zeinoddin, M., & Hashmi, S. (2018). Pistachio hull water-soluble polysaccharides as a novel prebiotic agent. *International Journal of Biological Macromolecules, 107*, 808–816. https://doi.org/10.1016/j.ijbiomac.2017.09.049

Association of Official Analytical Chemists. In AOAC (Ed.), *Methods of analysis. AOAC international* (twenty-first ed.), (2019) AOAC, Washington DC.

Bai, Y., Atluri, S., Zhang, Z., Gidley, M. J., Li, E., & Gilbert, R. G. (2021). Structural reasons for inhibitory effects of pectin on α-amylase enzyme activity and *in-vitro* digestibility of starch. *Food Hydrocolloids, 114*, Article 106581. https://doi.org/10.1016/j.foodhyd.2020.106581

Balaghi, S., Mohammadifar, M. A., Zargaraan, A., Gavlighi, H. A., & Mohammadi, M. (2011). Compositional analysis and rheological characterization of gum tragacanth exudates from six species of Iranian *Astragalus*. *Food Hydrocolloids, 25*(7), 1775–1784. https://doi.org/10.1016/j.foodhyd.2011.04.003

Benzie, I. F., & Strain, J. J. (1996). The ferric reducing ability of plasma (FRAP) as a measure of "antioxidant power": The FRAP assay. *Analytical Biochemistry, 239*(1), 70–76. https://doi.org/10.1006/abio.1996.0292

Bodart, M., de Peñaranda, R., Deneyer, A., & Flamant, G. (2008). Photometry and colorimetry characterisation of materials in daylighting evaluation tools. *Building and Environment, 43*(12), 2046–2058. https://doi.org/10.1016/j.buildenv.2007.12.006

Chen, T. T., Zhang, Z. H., Wang, Z. W., Chen, Z. L., Ma, H., & Yan, J. K. (2021). Effects of ultrasound modification at different frequency modes on physicochemical, structural, functional, and biological properties of citrus pectin. *Food Hydrocolloids, 113*, Article 106484. https://doi.org/10.1016/j.foodhyd.2020.106484

Chen, X., Qi, Y., Zhu, C., & Wang, Q. (2019). Effect of ultrasound on the properties and antioxidant activity of hawthorn pectin. *International Journal of Biological Macromolecules, 131*, 273–281. https://doi.org/10.1016/j.ijbiomac.2019.03.077

Chen, Y., Wang, Y., Xu, L., Jia, Y., Xue, Z., Zhang, M., … Chen, H. (2020). Ultrasound-assisted modified pectin from unripe fruit pomace of raspberry (*Rubus chingii* Hu): Structural characterization and antioxidant activities. *LWT-Food Science and Technology, 134*, Article 110007. https://doi.org/10.1016/j.lwt.2020.110007

Gavlighi, H. A., Michalak, M., Meyer, A. S., & Mikkelsen, J. D. (2013). Enzymatic depolymerization of gum tragacanth: Bifidogenic potential of low molecular weight oligosaccharides. *Journal of Agriculture and Food Chemistry, 61*(6), 1272–1278. https://doi.org/10.1021/jf304795f

Gavlighi, H. A., Tabarsa, M., You, S., Surayot, U., & Ghaderi-Ghahfarokhi, M. (2018). Extraction, characterization and immunomodulatory property of pectic polysaccharide from pomegranate peels: Enzymatic vs conventional approach. *International Journal of Biological Macromolecules, 116*, 698–706. https://doi.org/10.1016/j.ijbiomac.2018.05.083

Gharibzahedi, S. M. T., Smith, B., & Guo, Y. (2019). Ultrasound-microwave assisted extraction of pectin from fig (*Ficus carica* L.) skin: Optimization, characterization and bioactivity. *Carbohydrate Polymers, 222*, Article 114992. https://doi.org/10.1016/j.carbpol.2019.114992

Guo, Z., Ge, X., Yang, L., Gou, Q., Han, L., & Yu, Q. L. (2021). Utilization of watermelon peel as a pectin source and the effect of ultrasound treatment on pectin film properties. *LWT-Food Science and Technology, 147*, Article 111569. https://doi.org/10.1016/j.lwt.2021.111569

Ho, Y. Y., Lin, C. M., & Wu, M. C. (2017). Evaluation of the prebiotic effects of citrus pectin hydrolysate. *Journal of Food and Drug Analysis, 25*(3), 550–558. https://doi.org/10.1016/j.jfda.2016.11.014

Hosseini, S. S., Khodaiyan, F., Kazemi, M., & Najari, Z. (2019). Optimization and characterization of pectin extracted from sour orange peel by ultrasound assisted method. *International Journal of Biological Macromolecules, 125*, 621–629. https://doi.org/10.1016/j.ijbiomac.2018.12.096

Huebner, J., Wehling, R., Parkhurst, A., & Hutkins, R. (2008). Effect of processing conditions on the prebiotic activity of commercial prebiotics. *International Dairy Journal, 18*(3), 287–293. https://doi.org/10.1016/j.idairyj.2007.08.013

Kumar, M., Potkule, J., Tomar, M., Punia, S., Singh, S., Patil, S., … Kennedy, J. F. (2021). Jackfruit seed slimy sheath, a novel source of pectin: Studies on antioxidant activity, functional group, and structural morphology. *Carbohydrate Polymer Technologies and Applications, 2*, Article 100054. https://doi.org/10.1016/j.carpta.2021.100054

Liu, X., Le Bourvellec, C., & Renard, C. M. (2020). Interactions between cell wall polysaccharides and polyphenols: Effect of molecular internal structure. *Comprehensive Reviews in Food Science and Food Safety, 19*(6), 3574–3617. https://doi.org/10.1111/1541-4337.12632

Minzanova, S. T., Mironov, V. F., Arkhipova, D. M., Khabibullina, A. V., Mironova, L. G., Zakirova, Y. M., & Milyukov, V. A. (2018). Biological activity and pharmacological application of pectic polysaccharides: A review. *Polymers, 10*(12), 1407. https://doi.org/10.3390/polym10121407

Mirab, B., Gavlighi, H. A., Sarteshnizi, R. A., Azizi, M. H., & Udenigwe, C. C. (2020). Production of low glycemic potential sponge cake by pomegranate peel extract (PPE) as natural enriched polyphenol extract: Textural, color and consumer acceptability. *LWT-Food Science and Technology, 134*, Article 109973. https://doi.org/10.1016/j.lwt.2020.109973

Moreno-Vilet, L., Garcia-Hernandez, M., Delgado-Portales, R., Corral-Fernandez, N., Cortez-Espinosa, N., Ruiz-Cabrera, M., & Portales-Perez, D. (2014). *In vitro* assessment of agave fructans (*Agave salmiana*) as prebiotics and immune system activators. *International Journal of Biological Macromolecules, 63*, 181–187. https://doi.org/10.1016/j.ijbiomac.2013.10.039

Muñoz-Almagro, N., Montilla, A., Moreno, F. J., & Villamiel, M. (2017). Modification of citrus and apple pectin by power ultrasound: Effects of acid and enzymatic treatment. *Ultrasonics Sonochemistry, 38*, 807–819. https://doi.org/10.1016/j.ultsonch.2016.11.039

Nag, S., & Sit, N. (2018). Optimization of ultrasound assisted enzymatic extraction of polyphenols from pomegranate peels based on phytochemical content and antioxidant property. *Journal of Food Measurement and Characterization, 12*, 1734–1743. https://doi.org/10.1007/s11694-018-9788-2

Ogutu, F. O., & Mu, T. H. (2017). Ultrasonic degradation of sweet potato pectin and its antioxidant activity. *Ultrasonics Sonochemistry, 38*, 726–734. https://doi.org/10.1016/j.ultsonch.2016.08.014

Qiu, J., Zhang, H., & Wang, Z. (2019). Ultrasonic degradation of polysaccharides from *Auricularia auricula* and the antioxidant activity of their degradation products. *LWT-Food Science and Technology, 113*, Article 108266. https://doi.org/10.1016/j.lwt.2019.108266

Qiu, W. Y., Cai, W. D., Wang, M., & Yan, J. K. (2019). Effect of ultrasonic intensity on the conformational changes in citrus pectin under ultrasonic processing. *Food Chemistry, 297*, Article 125021. https://doi.org/10.1016/j.foodchem.2019.125021

Rubel, I. A., Pérez, E. E., Genovese, D. B., & Manrique, G. D. (2014). *In vitro* prebiotic activity of inulin-rich carbohydrates extracted from Jerusalem artichoke (*Helianthus tuberosus* L.) tubers at different storage times by *Lactobacillus paracasei*. *Food Research International, 62*, 59–65. https://doi.org/10.1016/j.foodres.2014.02.024

Seshadri, R., Weiss, J., Hulbert, G. J., & Mount, J. (2003). Ultrasonic processing influences rheological and optical properties of high-methoxyl pectin dispersions. *Food Hydrocolloids, 17*(2), 191–197. https://doi.org/10.1016/S0268-005X(02)00051-6

Sharifi, A., Hamidi-Esfahani, Z., Gavlighi, H. A., & Saberian, H. (2022). Assisted ohmic heating extraction of pectin from pomegranate peel. *Chemical Engineering and Processing- Process Intensification, 172*, Article 108760. https://doi.org/10.1016/j.cep.2021.108760

Tan, H. F., & Gan, C. Y. (2016). Polysaccharide with antioxidant, α-amylase inhibitory and ACE inhibitory activities from *Momordica charantia*. *International Journal of Biological Macromolecules, 85*, 487–496. https://doi.org/10.1016/j.ijbiomac.2016.01.023

Wang, C., Qiu, W. Y., Chen, T. T., & Yan, J. K. (2021). Effects of structural and conformational characteristics of citrus pectin on its functional properties. *Food Chemistry, 339*, Article 128064. https://doi.org/10.1016/j.foodchem.2020.128064

Xu, Y., Niu, X., Liu, N., Gao, Y., Wang, L., Xu, G., … Yang, Y. (2018). Characterization, antioxidant and hypoglycemic activities of degraded polysaccharides from blackcurrant (*Ribes nigrum* L.) fruits. *Food Chemistry, 243*, 26–35. https://doi.org/10.1016/j.foodchem.2017.09.107

Yan, J. K., Wang, C., Qiu, W. Y., Chen, T. T., Yang, Y., Wang, W. H., & Zhang, H. N. (2021). Ultrasonic treatment at different pH values affects the macromolecular, structural, and rheological characteristics of citrus pectin. *Food Chemistry, 341*, Article 128216. https://doi.org/10.1016/j.foodchem.2020.128216

Yang, X., Nisar, T., Hou, Y., Gou, X., Sun, L., & Guo, Y. (2018). Pomegranate peel pectin can be used as an effective emulsifier. *Food Hydrocolloids, 85*, 30–38. https://doi.org/10.1016/j.foodhyd.2018.06.042

Yeung, Y. K., Kang, Y. R., So, B. R., Jung, S. K., & Chang, Y. H. (2021). Structural, antioxidant, prebiotic and anti-inflammatory properties of pectic oligosaccharides hydrolyzed from okra pectin by Fenton reaction. *Food Hydrocolloids, 118*, Article 106779. https://doi.org/10.1016/j.foodhyd.2021.106779

Zhang, H., Cui, S. W., Nie, S. P., Chen, Y., Wang, Y. X., & Xie, M. Y. (2016). Identification of pivotal components on the antioxidant activity of polysaccharide extract from *Ganoderma atrum*. *Bioactive Carbohydrates and Dietary Fibre, 7*(2), 9–18. https://doi.org/10.1016/j.bcdf.2016.04.002

Zhang, L., Ye, X., Ding, T., Sun, X., Xu, Y., & Liu, D. (2013). Ultrasound effects on the degradation kinetics, structure and rheological properties of apple pectin. *Ultrasonics Sonochemistry, 20*(1), 222–231. https://doi.org/10.1016/j.ultsonch.2012.07.021

Zhang, L., Ye, X., Xue, S. J., Zhang, X., Liu, D., Meng, R., & Chen, S. (2013). Effect of high-intensity ultrasound on the physicochemical properties and nanostructure of citrus pectin. *Journal of the Science of Food and Agriculture, 93*(8), 2028–2036. https://doi.org/10.1002/jsfa.6011

Zhang, S., Hu, H., Wang, L., Liu, F., & Pan, S. (2018). Preparation and prebiotic potential of pectin oligosaccharides obtained from citrus peel pectin. *Food Chemistry, 244*, 232–237. https://doi.org/10.1016/j.foodchem.2017.10.071

Zhou, F., Jiang, X., Wang, T., Zhang, B., & Zhao, H. (2018). *Lycium barbarum* polysaccharide (LBP): A novel prebiotics candidate for *Bifidobacterium* and *Lactobacillus*. *Frontiers in Microbiology, 9*, 1034. https://doi.org/10.3389/fmicb.2018.01034

Zhu, R., Wang, C., Zhang, L., Wang, Y., Chen, G., Fan, J., … Ning, C. (2019). Pectin oligosaccharides from fruit of *Actinidia arguta*: Structure-activity relationship of prebiotic and antiglycation potentials. *Carbohydrate Polymers, 217*, 90–97. https://doi.org/10.1016/j.carbpol.2019.04.032